



Advancing precision medicine in immunoglobulin light-chain amyloidosis: a novel prognostic model incorporating multi-organ indicators

Yan Xing¹ · Xiayin Li¹ · Jin Zhao¹ · Hao Wu¹ · Lijuan Zhao¹ · Wanting Zheng¹ · Shiren Sun¹

Received: 3 January 2024 / Accepted: 17 April 2024 / Published online: 14 May 2024
© The Author(s), under exclusive licence to Società Italiana di Medicina Interna (SIMI) 2024

Abstract

To develop a more accurate prognostic model that incorporates indicators of multi-organ involvement for immunoglobulin light-chain (AL) Amyloidosis patients. Biopsy-proven AL amyloidosis patients between January 1, 2012, and February 28, 2023, were enrolled and randomly divided into a training set and a test set at a ratio of 7:3. Prognostic indicators that comprehensively cover cardiac, renal, and hepatic involvement were identified in the training set by random survival forest (RSF). Then, RSF and Cox models were established. The Concordance index (C-index) and integrated brier scores (IBS) were applied to evaluate the models' performance in the test set. Besides, the net reclassification index (NRI) and integrated discrimination improvement (IDI) were calculated. A total of 173 eligible patients were included. After a median follow-up of 25.9 (9.2, 50.3) months, 48 (27.7%) patients died. Creatine kinase-MB, estimated glomerular filtration rate ≤ 50 mL/min/1.73 m², interventricular septum ≥ 15 mm, ejection fraction, alanine aminotransferase and Live involved were selected to develop prediction models. The RSF model based on the above indicators achieved C-index and IBS values of 0.834 (95% CI 0.725–0.915) and 0.151 (95% CI 0.1402–0.181), respectively. At last, the NRI and IDI of the RSF model were 0.301 (95% CI 0.048–0.546, $P=0.012$) and 0.157 (95% CI 0.041–0.269, $P<0.001$) at 5-year by comparing the RSF model with the Cox model which is based on the Mayo 2012 staging system. The RSF model that incorporates indicators of multi-organ involvement had a great performance, which may be helpful for physicians' decision-making and more accurate overall survival prediction.

Keywords Amyloid · Immunoglobulin light-chain amyloidosis · Machine learning · Prognosis · Survival

Introduction

Immunoglobulin light-chain (AL) amyloidosis is a progressive disease characterized by the deposition of amyloid fibrillar in tissues, which is derived from the monoclonal immunoglobulin light chain produced by clonal plasma cells [1]. It is estimated that around 74,000 AL amyloidosis patients were diagnosed globally in the past 20 years prior to 2018, and the estimated incidence rate was 10 cases per

million population with an increase in disease prevalence of 12% per year [2, 3]. According to previous research, the outcome of AL amyloidosis patients is improved with the median overall survival (OS) from 1.4 to 4.6 years [4]. However, the largest real-world study of AL amyloidosis patients in Europe indicated that the early mortality (within 3 months after therapy) was 13.4% and did not improve pre- and post-2010 despite the therapeutic advances [5]. More than one-third of patients died after diagnosis of AL amyloidosis within one year [6]. Accurately predicting the patient's outcome and providing appropriate treatment are crucial.

The current OS prediction for AL amyloidosis is based on the indicators of cardiac involvement [7]. The Mayo 2004 staging system, which only relies on cardiac biomarkers, is utilized for assessing the severity of AL amyloidosis patients with advanced cardiac involvement and continues to be employed in clinical investigations and practice guidelines up to now [8–10]. The Mayo 2012 staging system, which

Yan Xing, Xiayin Li, and Jin Zhao have contributed equally to this work and share the first authorship.

✉ Shiren Sun
sunshiren@medmail.com.cn

¹ Department of Nephrology, Xijing Hospital, The Fourth Military Medical University, No.127 Chang Le West Road, Xi'an 710032, Shaanxi, China

incorporates serum free light chain measurements (FLC) into Mayo 2004 staging system, has been hypothesized to have a more precise prediction of the long-term prognosis for patients with AL amyloidosis [11]. However, as a multi-system disease, the prognosis of AL amyloidosis patients is not only affected by a single organ, which is supported by the increasing number of proven risk factors for AL amyloidosis [12]. It is considered significant to develop comprehensive, multi-disciplinary approaches to clinical diagnosis, treatment and prognosis for AL amyloidosis patients. Random survival forest (RSF), a machine learning algorithm that combines random forest with survival analysis and can integrate high-dimensional data, has shown promising performance in patients with other diseases [13, 14]. To accurately predict OS for AL amyloidosis patients, the goal of this study was to identify key indicators of multi-organ involvement and then to develop a prognostic model based on the RSF and validate its performance.

Methods

Data collection

The patients diagnosed at Xijing hospital from January 1, 2012 to February 28, 2023 were included in this study. The confirmation of AL amyloidosis is based on 2023 National Comprehensive Cancer Network guidelines [1]. Exclusion criteria were as follows: (1) patients' pathology reports, such as renal or fat biopsy, were missing; (2) patients who were secondary to multiple myeloma according to the criteria by the International Myeloma Working Group [15]; (3) patients whose clinical data of the difference between involved and uninvolved free light chain (dFLC), N-Terminal pro-Brain Natriuretic Peptide (NT-proBNP), cardiac troponin T (cTnT) and cardiac troponin I (cTnI) were unavailable when the confirmation of AL amyloidosis; (4) patients with ejection fraction (EF) < 45% at the confirmation of AL amyloidosis; (5) patients whose follow-up time less than 3 months unless they died due to all causes. Involvement of organs was assessed according to the 10th International Symposium on Amyloid and Amyloidosis [16]. The eligible patients' clinical data at the time of diagnosis by biopsy, including demographic characteristics, clinical indicators, pathological characteristics and treatment strategies, were gathered. The OS was defined as the time between the confirmation of AL amyloidosis and death or the last follow-up until May 31, 2023. This study was authorized by Xijing Hospital's ethics committees and review board, and informed consent was not required because of the nature of the retrospective study. Transparent Reporting of a Multivariable Prediction Model

for Individual Prognosis or Diagnosis reporting guidelines was followed in this study (Supplemental Table 1) [17].

Statistical analysis

The continuous variables were presented by mean (standard deviation) or median (interquartile range), and the categorical variables were expressed as number (frequencies). The *t* test or the Mann–Whitney *U* test was performed to compare continuous variables, and the χ^2 test or the Fisher exact test was applied for categorical variables. All statistical analyses were finished by SPSS software package version 26.0 (IBM, Armonk, New York) and 2-sided *P*-values less than 0.05 were considered statistically significant. The model development and assessment were performed by R version 4.3.0 (R Project for Statistical Computing).

Model development

Variables' missing value was imputed by “missForest 1.5” package, but the variable that missed exceed 10% should be deleted. To reduce confounding, continuous variables with Spearman's correlation coefficients greater than 0.4 would also be deleted. After that, all data were randomly divided into a training set and a test set at a ratio of 7:3. The training set was used to assess the variable importance (VIMP), and 95% confidence interval (CI) of VIMP was calculated by applying the bootstrapping resampling method with 1000 repetitions. The variables with mean VIMP more than 0.03 were selected for developing the final RSF model by “randomForestSRC 3.2.1” package. The ideal hyperparameter was identified by the grid search method.

Model validation

The Concordance index (C-index) and the area under the receiver operating characteristic curve (AUC) were calculated to evaluate the model's discrimination. Integrated brier score (IBS) and Calibration Curve were used to evaluate the model's calibration. To ensure accuracy, the bootstrap method with 1000 repetitions was performed to calculate the 95% CI of C-index and IBS of prediction models.

Cox models, which were based on the variables with mean VIMP more than 0.03, Mayo 2004 staging system and Mayo 2012 staging system, were developed to validate the Superiority–Inferiority of the RSF model. Decision Curve Analysis was also performed to confirm the clinical benefits of different models. Besides, Net reclassification improvement (NRI) and integrated discrimination improvement (IDI) between models were calculated.

Table 1 Clinical characteristics of patients

Characteristics	All patients (N= 173)	Training set (N= 121)	Test set (N= 52)	p
Age (years)	58.0 ± 9.4	58.6 ± 9.1	56.8 ± 9.8	0.203
Male	106 (61.3)	76 (62.8)	30 (57.7)	0.526
BMI (kg/m ²) ^a	22.6 (21.1, 24.6)	23.0 (21.3, 24.7)	22.5 (20.7, 24.2)	0.304
SBP (mmHg)	111.0 (94.0, 124.0)	112.0 (96.0, 123.5)	106.5 (92.5, 124.8)	0.527
DBP (mmHg)	69.0 (60.0, 81.5)	70.0 (60.0, 80.5)	67.0 (60.3, 82.8)	0.657
Hb (g/L)	130.0 (117.0, 146.0)	132.0 (116.5, 146.0)	127.5 (117.3, 140.8)	0.346
WBC (10 ⁹ /L)	7.4 (5.8, 9.9)	7.4 (5.8, 9.7)	7.3 (5.8, 10.0)	0.642
PLT (10 ⁹ /L)	229.0 (173.5, 311.5)	227.0 (177.0, 296.5)	245.5 (172.3, 322.3)	0.639
ALT (IU/L)	20.0 (14.0, 29.0)	21.0 (15.0, 31.0)	18.5 (14.0, 28.0)	0.268
AST (IU/L)	22.0 (17.0, 32.0)	22.0 (17.5, 33.0)	23.5 (17.0, 30.5)	0.999
ALB (g/L)	25.8 (20.3, 32.9)	25.2 (20.6, 31.4)	27.2 (19.5, 34.7)	0.306
TBIL (μmol/L)	9.1 (6.9, 12.7)	9.1 (6.9, 11.9)	9.4 (6.1, 13.9)	0.732
ALP (IU/L)	74.0 (61.0, 105.5)	74.0 (61.0, 102.5)	73.5 (60.3, 107.5)	0.836
CHO (mmol/L)	5.8 (4.4, 8.0)	5.7 (4.5, 8.0)	6.0 (4.1, 8.4)	0.719
CRE (μmol/L)	77.0 (63.5, 99.0)	81.0 (65.0, 100.5)	73.5 (62.3, 90.8)	0.177
eGFR (mL/min/1.73 m ²) ^b	86.0 (64.5, 100.9)	84.4 (63.3, 98.7)	95.9 (68.9, 102.3)	0.092
UA (μmol/L)	326.0 (268.3, 402.0)	328.0 (265.0, 401.0)	323.0 (281.0, 418.8)	0.773
UTP (mg/24 h)	3276.0 (1490.0, 5322.5)	3528.0 (1637.0, 5600.0)	2174.0 (1278.0, 4478.5)	0.111
K (mmol/L)	4.1 (3.7, 4.4)	4.1 (3.8, 4.4)	4.0 (3.7, 4.3)	0.483
Na (mmol/L)	141.7 (138.9, 143.7)	141.6 (138.8, 143.8)	142.1 (139.0, 143.4)	0.887
Ca (mmol/L)	2.1 (1.9, 2.2)	2.1 (1.9, 2.2)	2.1 (2.0, 2.2)	0.306
CO ₂ (mmol/L)	25.6 (23.8, 27.5)	25.6 (23.8, 27.6)	25.9 (23.8, 27.5)	0.888
Fib (g/L)	4.2 (3.1, 5.2)	4.2 (3.1, 5.2)	4.0 (3.0, 5.2)	0.650
TT (s)	18.4 (17.2, 19.9)	18.5 (17.3, 20.0)	18.3 (16.8, 19.7)	0.352
DDi (mg/L)	0.9 (0.5, 2.3)	0.9 (0.5, 2.2)	0.8 (0.5, 2.4)	0.867
κ FLC (mg/L)	19.2 (12.4, 34.2)	20.6 (13.9, 34.5)	14.9 (11.1, 30.4)	0.116
λ FLC (mg/L)	115.0 (46.9, 171.2)	113.4 (43.2, 188.7)	115.8 (48.3, 150.4)	0.515
λ Subtype	144 (83.2)	101 (83.5)	43 (82.7)	0.900
rFLC	0.2 (0.1, 0.4)	0.2 (0.1, 0.4)	0.2 (0.1, 0.5)	0.775
dFLC (mg/L)	99.8 (45.5, 164.4)	99.4 (45.9, 173.7)	101.1 (44.3, 151.2)	0.901
CK-MB (ng/mL)	2.3 (1.2, 4.4)	2.3 (1.2, 4.1)	2.5 (1.1, 4.6)	0.867
NT-proBNP (pg/mL)	890.2 (204.4, 3450.0)	853.3 (217.7, 3274.0)	1446.5 (169.1, 4153.3)	0.775
cTnT (ng/mL)	0.03 (0.01, 0.07)	0.03 (0.01, 0.07)	0.03 (0.01, 0.09)	0.756
cTnI (ng/mL)	0.05 (0.01, 0.13)	0.04 (0.01, 0.13)	0.05 (0.01, 0.13)	0.937
EF	58 (55, 60)	58 (55, 60)	58 (55, 60)	0.687
IVS (mm)	11.0 (10.0, 13.5)	11.0 (10.0, 13.5)	11.5 (10.0, 13.4)	0.536
Therapy				
None	11 (6.4)	8 (6.7)	3 (5.8)	1.000
CTD or MD or RD	72 (41.6)	48 (39.7)	24 (46.2)	0.428
BD or Dara or Dara + BD	90 (52.0)	65 (53.6)	25 (48.0)	0.496
Time before diagnosis (months) ^c	5.0 (2.0, 12.0)	5.0 (2.0, 12.0)	6.0 (2.3, 16.5)	0.221
Number of organs involved	2.0 (1.0, 2.0)	2.0 (1.0, 2.0)	2.0 (1.0, 2.0)	0.952
Organs involved				
Kidney involvement	166 (95.9)	116 (95.9)	50 (96.2)	1.000
Heart involvement	103 (59.5)	72 (59.5)	31 (59.6)	0.989
Live involvement	17 (9.8)	12 (9.9)	5 (9.6)	0.951
Other organs involvement ^d	4 (2.3)	3 (2.5)	1 (1.9)	1.000
Mayo 2004				
I stage	43 (24.9)	28 (23.1)	15 (28.8)	0.426
II stage	24 (13.9)	19 (15.7)	5 (9.6)	0.288

Table 1 (continued)

Characteristics	All patients (N=173)	Training set (N=121)	Test set (N=52)	p
III stage	106 (61.2)	74 (61.2)	32 (61.6)	0.962
Mayo 2012				
I stage	79 (45.7)	55 (45.5)	24 (46.2)	0.933
II stage	32 (18.5)	26 (21.5)	6 (11.5)	0.122
III stage	47 (27.2)	27 (22.3)	20 (38.5)	0.029
IV stage	15 (8.6)	13 (10.7)	2 (3.8)	0.237
Follow-up time (months)	25.9 (9.2, 50.3)	27.5 (13.2, 48.9)	14.6 (5.95, 55.8)	0.193
Death	48 (27.7)	31 (25.6)	17 (32.7)	0.341

BMI body mass index, *SBP* systolic blood pressure, *DBP* diastolic blood pressure, *Hb* hemoglobin, *WBC* white blood cell, *PLT* blood platelet, *ALT* alanine aminotransferase, *AST* aspartate aminotransferase, *ALB* albumin, *TBIL* total bilirubin, *ALP* alkaline phosphatase, *CHO* cholesterol, *CRE* creatinine, *eGFR* estimated glomerular filtration rate, *UA* uric acid, *UTP* urinary total protein, *Fib* fibrinogen, *TT* thrombin time, *DDi* d-dimer, *FLC* free light chain, *iFLC* involved free light chain, *rFLC* ratio of κ FLC/ λ FLC, *dFLC* difference between involved FLC and uninvolved FLC, *CK-MB* creatine kinase-MB, *NT-proBNP* n-terminal pro-brain natriuretic peptide, *cTnT* cardiac troponin t, *cTnI* cardiac troponin I, *EF* ejection fraction, *IVS* interventricular septum, *CTD* cyclophosphamide + thalidomide + dexamethasone, *MD* melphalan + dexamethasone, *RD* lenalidomide + dexamethasone, *BD* bortezomib + dexamethasone, *Dara* daratumumab

^aBMI was calculated as weight/height²

^beGFR was calculated by the chronic kidney disease epidemiology collaboration (CKD-EPI) equation

^cTime before diagnosis was the time between the onset of symptoms and the confirmation of amyloid light-chain amyloidosis

^dOther organs including the gastrointestinal tract or peripheral nervous system

3. Results

Characteristics of patients

A total of 173 patients were included (Fig. 1). The mean age was 58 ± 9.4 years old. 106 (61.3%) patients were male. 144 (83.2%) patients had lambda amyloidogenic light chains. According to Mayo 2004 staging system, 43 (24.9%), 24

(13.9%) and 106 (61.2%) patients were in the I, II and III stage. 79 (45.7%), 32 (18.5%), 47 (27.2%) and 15 (8.6%) patients were in the I, II, III and IV stage based on Mayo 2012 staging system. Patients with renal and cardiac involvement were 166 (95.9%) and 103 (59.5%), respectively. 104 (60.1%) patients had more than two organs involved. After a median follow-up of 25.9 (9.2, 50.3) months, 48 (27.7%) AL amyloidosis patients died (Table 1).

Fig. 1 Flowchart of this study. AL amyloidosis, immunoglobulin light-chain amyloidosis, EF ejection fraction

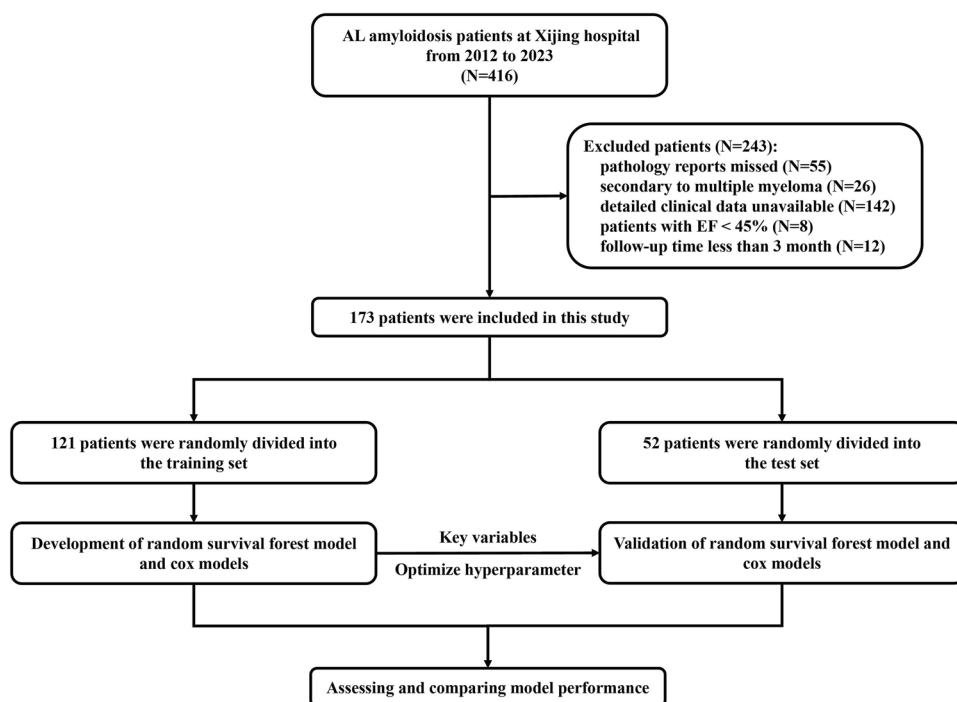


Table 2 The concordance index and Integrated brier score of all prediction models

Prediction models	Training set		Test set	
	C-index (95% CI)	IBS (95% CI)	C-index (95% CI)	IBS (95% CI)
RSF model	0.843 (0.761–0.898)	0.106 (0.104–0.109)	0.834 (0.725–0.915)	0.151 (0.140–0.181)
Cox model A	0.769 (0.661–0.844)	0.136 (0.135–0.137)	0.856 (0.727–0.913)	0.132 (0.119–0.164)
Cox model B	0.794 (0.716–0.855)	0.1472 (0.142–0.156)	0.860 (0.716–0.924)	0.122 (0.116–0.134)
Cox model C	0.820 (0.738–0.875)	0.150 (0.145–0.158)	0.810 (0.682–0.895)	0.195 (0.153–0.245)
Cox model D	0.792 (0.706–0.850)	0.146 (0.141–0.156)	0.856 (0.733–0.928)	0.122 (0.1164–0.132)

C-index the concordance index, IBS integrated brier score, 95% CI 95% confidence interval, RSF random survival forests

Creatine kinase-MB, estimated glomerular filtration rate ≤ 50 mL/min/1.73 m², interventricular septum ≥ 15 mm, ejection fraction, alanine aminotransferase and Live involved were adopted to develop RSF model and Cox model A; Cox model B was based on NT-proBNP and cTnT; Cox model C was based on NT-proBNP and cTnI; Cox model D was based on NT-proBNP, cTnT and dFLC

The C-index of 0.5 implies a meaningless model while the C-index above 0.75 indicates a meaningful model. The lower IBS value indicates a smaller difference between the prediction of models and the actual situation. A value below 0.25 means that the model is useful.

Model development

49 continuous variables and 23 categorical variables were included in our study (Supplemental Table 2). Previously reported thresholds were used to dichotomize categorical variables. 13 variables had missing values but no one of them missed exceed 10% and no statistically significant were found before and after imputation (Supplemental Table 3). After deleting confounding variables, 23 continuous variables were left (Supplemental Fig. 1), and were evaluated by RSF together with 23 categorical variables. At last, 34 variables could be used to develop the RSF model due to their mean VIMP > 0 (Fig. 2). Creatine kinase-MB (CK-MB), estimated glomerular filtration rate (eGFR) ≤ 50 mL/min/1.73 m², interventricular septum (IVS) ≥ 15 mm, EF, alanine aminotransferase (ALT) and Live involved were the key indicators with a mean VIMP more than 0.03. The ntree for the final RSF model was set to 800. According to grid search, the optimize mtry and nodesize were 1 and 8, respectively (Supplemental Fig. 2).

Model performance

Discrimination

The C-index of all prediction models were presented in Table 2. In the training set, the RSF model had the highest C-index with 0.843 (95% CI 0.761–0.898) and the Cox model which was based on the same variables was the lowest with 0.769 (95% CI 0.661–0.844). The C-index of Cox models which were based on Mayo staging system were satisfactory. In the test set, the RSF model's C-index dropped slightly to 0.834 (95% CI 0.725–0.915), but the C-index of Cox model which was based on the same factors rose to 0.856 (95% CI 0.727–0.913). Besides, it was notable that the C-index of Cox model which was based on NT-proBNP and cTnI was the lowest with 0.810 (95% CI 0.682–0.895).

The receiver operating characteristic curves of all models were also plotted (Fig. 3). In the training set (Fig. 3A), AUCs of the RSF model at 1-, 3- and 5-year were 0.875, 0.882 and 0.852 and the AUCs of Cox model which was based on the same factors were 0.800 0.794 and 0.723. RSF model's AUCs were the highest among all prediction models at 3- and 5-year. In the test set (Fig. 3B), the AUCs of RSF model at 1-, 3- and 5-year were 0.790, 0.870 and 0.895, and the Cox model which was based on the same factors had the AUCs of 0.834, 0.890 and 0.905. The Cox model which was based on NT-proBNP and cTnI had the lowest AUC with 0.868 and 0.852 at 3- and 5-year.

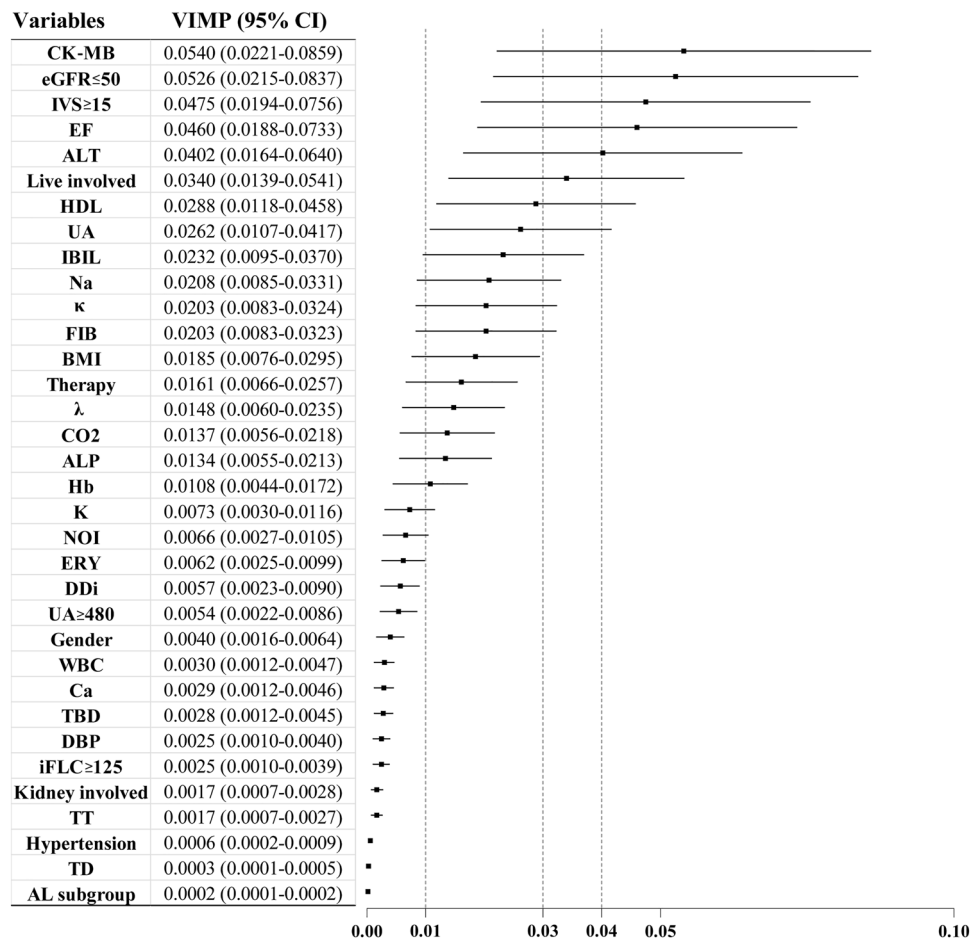


Fig. 2 Variable importance of indicators favourable for developing model. VIMP variable importance, CK-MB creatine kinase-MB, eGFR estimated glomerular filtration rate, IVS interventricular septum, EF ejection fraction, ALT alanine aminotransferase, HDL high-density lipoprotein, UA uric acid, IBIL indirect bilirubin, Fib Fibrinogen, BMI body mass index, ALP alkaline phosphatase, Hb Hemoglobin, NOI number of organs involved, ERY erythrocyte, DDi D-Dimer, WBC white blood cell, TBD time before diagnosis, DBP diastolic blood pressure, iFLC involved free light chain, TT

thrombin time, TD thyroid dysfunction. To reduce confounding, 26 continuous variables were removed. Then, the VIMP of the last 23 continuous variables and 23 categorical variables were evaluated by the RSF algorithm. 12 variables were also removed due to their $VIMP \leq 0$, which means they were unfavorable for developing model. Eventually, 34 variables were selected. As we can see, the CK-MB, $eGFR \leq 50$ mL/min/1.73 m², $IVS \geq 15$ mm, EF, ALT and Live involvement were identified as the top six factors

Calibration

All models with low IBS showed great calibration ability (Table 2). The RSF model's IBS was 0.106 (95% CI 0.104–0.109) in the training set and 0.151 (95% CI 0.140–0.181) in the test set. The IBS of Cox model which was based on the same factors were 0.136 (95% CI 0.135–0.137) and 0.132 (95% CI 0.119–0.164) in the training set and test set, respectively. However, it was notable that the Cox model which was based on NT-proBNP and cTnI had the highest IBS in both the training set and test set. The calibration curves of RSF model were displayed (Supplemental Fig. 3), which confirmed the great performance of RSF model.

Decision Curve Analysis

In the training set, the RSF model was more beneficial than other Cox models at 1-, 3- and 5-year (Supplemental Fig. 4A). In the test set (Supplemental Fig. 4B), the benefits of Cox model which was based on NT-proBNP and cTnI were consistently the least compared with other prediction models.

NRI and IDI

All data was integrated to calculate NRI and IDI between the RSF model and other Cox models (Supplemental Table 4 and Supplemental Table 5). The Cox model which

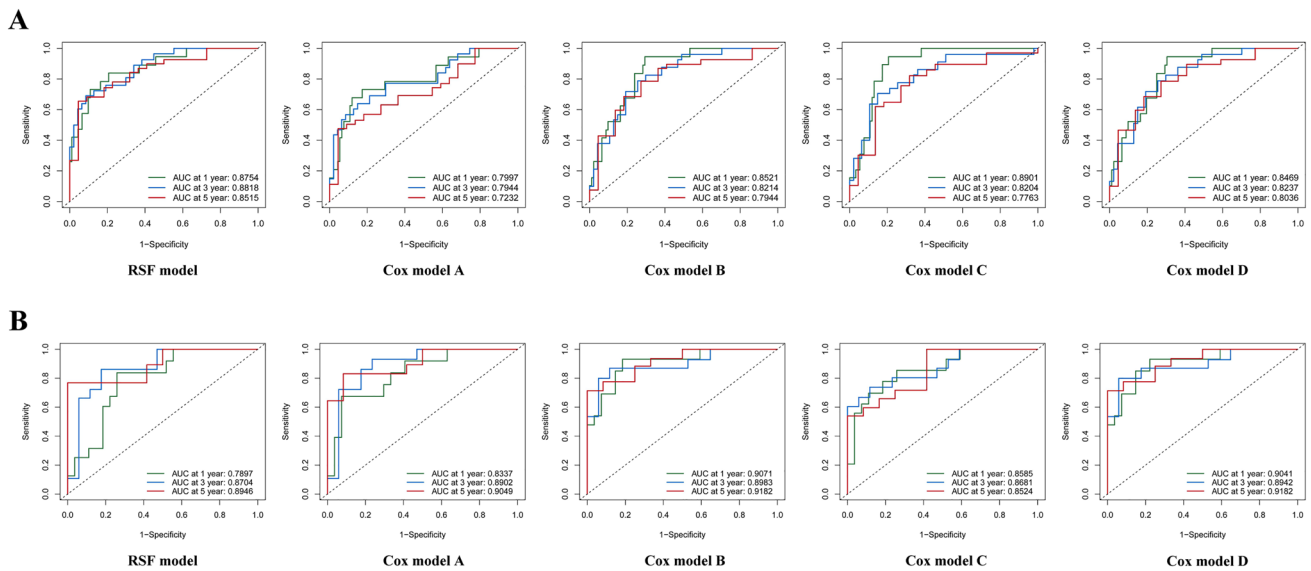


Fig. 3 The receiver operating characteristic curve of all prediction models. (A) are the receiver operating characteristic curves (ROC) in the training set. (B) are the ROC in the test set. Creatine kinase-MB, estimated glomerular filtration rate ≤ 50 mL/min/1.73 m², interventricular septum ≥ 15 mm, ejection fraction, alanine aminotransferase and Live involved are adopted to develop random survival forest

was based on NT-proBNP, cTnT and dFLC was used as the reference model. At 1-year, the RSF model's NRI and IDI were 0.229 (95% CI -0.013 – 0.474 , $P = 0.064$) and 0.064 (95% CI -0.075 – 0.212 , $P = 0.406$), which indicated the RSF model performed just as well as the Cox model which was based on NT-proBNP, cTnT and dFLC. However, the NRI and IDI of the Cox model which was based on NT-proBNP and cTnI were -0.457 (95% CI -0.660 – 0.302 , $P < 0.01$) and -0.210 (95% CI -0.320 – 0.108 , $P < 0.01$), which meant the relatively poor performance. At 3-year, the NRI and IDI of the RSF model was 0.272 (95% CI 0.059–0.506, $P = 0.014$) and 0.126 (95% CI 0.008–0.251, $P = 0.032$). At 5-year, the NRI and IDI of the RSF model were 0.301 (95% CI 0.048–0.546, $P = 0.024$) and 0.157 (95% CI 0.041–0.269, $P < 0.01$). These results indicated the RSF model had superior performance than the Cox model which was based on NT-proBNP, cTnT and dFLC. Meanwhile, the poor performance of Cox model which was based on NT-proBNP and cTnI was still evident at 3- and 5-year ($P < 0.01$).

The effect of treatment options on RSF model

In addition, we verified the effect of treatment options on RSF model. We grouped patients' treatment options into five categories (Supplemental Table 6). The RSF model was developed by combining patients' treatment options with the other six variables identified in our study (RSF-therapy). The C-index was 0.848 (95% CI 0.717–0.923) and the IBS of

(RSF) model and Cox model A. Cox model B was based on N-Terminal pro-Brain Natriuretic Peptide (NT-proBNP) and cardiac troponin T (cTnT). Cox model C was based on NT-proBNP and cardiac troponin I. Cox model D was based on NT-proBNP, cTnT and the difference between involved and uninvolved free light chains

RSF-therapy was 0.138 (95% CI 0.126–0.172) in the test set (Supplemental Table 7). However, the AUCs of RSF-therapy were lower than those of our original RSF model at 5-year (Supplemental Fig. 5). To validate the Superiority–Inferiority of the RSF therapy compared with our original RSF model, the NRI and IDI of RSF-therapy were calculated (Supplemental Table 8). As we can see, NRI and IDI at 1-, 3- and 5-year ($P < 0.05$) indicated RSF-therapy had superior performance than our original RSF model.

Discussion

The main findings of our research are as follows. First, six routinely used indicators were identified with a significant impact on all-cause death for AL amyloidosis patients, which were CK-MB, eGFR ≤ 50 mL/min/1.73 m², IVS ≥ 15 mm, EF, ALT, and Live involved. Second, the RSF model that incorporates above indicators of multi-organ involvement had great performance. Third, the Cox model which was based on NT-proBNP and cTnI was inferior to other models.

The outcome of AL amyloidosis patients mainly depends on whether cardiac is involved. However, traditional indicators such as NT-proBNP, cTnT, and cTnI were removed due to the high correlations among cardiac markers. At last, the CK-MB, EF, and IVS ≥ 15 mm were identified as crucial cardiac indicators. Previous studies have confirmed

that an increased mortality rate was related to the elevation of CK-MB after percutaneous coronary intervention [18], and elevated CK-MB may predict the adverse outcome of patients with coronavirus disease 19 [19]. However, the prognostic value of CK-MB in AL amyloidosis is not clear yet. According to previous studies, FLCs can induce increased reactive oxygen species production in cardiomyocytes, followed by apoptosis and then lead to impaired heart function [20], which may cause the release of CK-MB from cardiomyocytes in AL amyloidosis patients.

AL amyloidosis patients often had heart failure with preserved EF, and experienced decreased EF in the advanced stage of disease. Meanwhile, IVS gradually thickens due to the deposition of amyloid and then leads to a poor outcome once the IVS exceeds the normal range significantly. Besides, the thickness of IVS was found to be significantly associated with high NT-proBNP levels [21], which is the main marker in the Mayo staging system. To early and accurately recognize pathological changes that may lead to decreased EF with thickened LVS in AL amyloidosis, Gallium-68-labeled fibroblast activation protein inhibitor 04 (68 Ga-FAPI-04) had demonstrated its significant correlations with EF and IVS [22]. Furthermore, cardiac 68 Ga-FAPI-04 PET/CT also proved its great potential in the diagnosis and prognosis of AL amyloidosis patients [22]. Identifying the changes in EF and IVS early may prevent long-term death in AL amyloidosis.

Hepatic involvement is found in approximately 20% of AL amyloidosis patients. The 5- and 10-year survival rates of those patients are less than 16.9 and 6.6% in the past [23, 24]. Even with the advent of the new therapy, the prognosis of patients with hepatic involvement is still poor. For patients with hepatic involvement, hepatocytes may be compressed by excessive amyloid deposits, which will cause them to atrophy and then to hepatic dysfunction [25]. Chronic heart failure due to cardiac amyloidosis also influenced hepatic dysfunction [26]. Therefore, alkaline phosphatase (ALP) and total bilirubin were found to be independent prognostic factors for those patients. In our study, total bilirubin was also removed, and indirect bilirubin with ALP was identified as prognostic factors but were not selected to develop models due to their relatively lower VIMP. Eventually, ALT that be found as a predictor of mortality in a previous study [27], was selected to develop the prediction model.

In patients with renal involvement, the decreased eGFR appeared in the stage of irreversible damage of FLCs to the kidney. The decreased eGFR seems to be related to prerenal kidney injury brought on by cardiac involvement [28]. According to previous studies, 50 mL/min/1.73 m² of eGFR and 5 g of urinary total protein (UTP) could be considered the key threshold for adverse outcomes [29]. In our study, only eGFR \leq 50 mL/min/1.73 m² at the time of biopsy was identified as a key indicator (VIMP more than 0.03), which

confirmed the significance of eGFR to all-cause death. That was also supported by other studies that impaired renal function negatively affects overall survival, but proteinuria does not [28]. Besides, amyloid deposition in the kidney not only can lead to renal dysfunction but also accelerate the pre-existent renal insufficiency. However, the exact time when renal dysfunction began to develop was not known because a decline in eGFR was hard to perceive by patients. In this study, we included the time interval between the onset of disease-related symptoms and a definitive diagnosis of AL amyloidosis (TBD), and the TBD was also identified as a key variable that was beneficial for RSF model development (VIMP more than 0) (Fig. 2). This suggested that early diagnosis is crucial for patients, which also implied the importance of early intervention, such as maintaining normal renal function by reducing the damage of amyloid or other treatments.

The comprehensive and interdisciplinary approaches for AL amyloidosis are developing. Jimenez-Zepeda et al. presented a multifaceted, interdisciplinary algorithm aimed at diagnosing amyloidosis, with the potential to streamline diagnostic processes, enable prompt and accurate interventions, and ultimately improve patient outcomes [30]. Yan et al. developed a novel clinical prognostic staging system for individuals with AL amyloidosis by integrating plasma cell-related characteristics with cardiac-renal-hepatic parameters, thereby enhancing risk stratification [31]. However, as mentioned in the literature above, there are regional variations in the availability of resources for prognostic testing. The existing staging systems do not provide precise survival estimates and variations in threshold values for the same indicator may also cause some interference in clinical practice. Furthermore, Cox proportional hazards analysis is deficient in making full use of voluminous, messy and complex clinical data. Besides, the linear relationship between the hazard and variables, and proportional hazards assumption may not be applicable for some time-to-event data, which may limit the performance of Cox models. However, the RSF model can avoid the restrictions mentioned above [32].

Most importantly, the RSF model shows great performance in discrimination, calibration and clinical utility. In the test set, the C-index of the RSF model was 0.834 (95% CI 0.725–0.915). Meanwhile, the AUCs of the RSF model were also satisfactory. The IBS of the RSF model was also relatively lower. By comparing the RSF model to the Cox model which is based on the Mayo 2012 staging system, we found both the NRI and IDI of the RSF model were statistically significant improvements at 3- and 5-year, which implied a better performance. Besides, the DCA of the RSF model also presented its benefits. In contrast, the Cox model which was based on NT-proBNP and cTnI showed relatively poor performance with the lowest C-index, the highest IBS, and the most limited DCA, which was consistent with

previous research that the survival status of AL amyloidosis patients could not be comparatively accurately divided by NT-proBNP combined with cTnI [33, 34].

By comparing RSF therapy with original RSF model, we speculated that incorporating treatment options in RSF model can effectively predict the prognosis of AL amyloidosis patients. However, the cohort of patients participating in our study who opted for daratumumab-based therapy was limited in sample size. Considering the robust effect of daratumumab-based therapy in AL amyloidosis patients and its potential adoption by a large number of patients in the future [8, 9, 35, 36], the performance of RSF-therapy is likely to be further improved.

Our research also has several limitations. First, due to the rarity of AL amyloidosis, the number of patients included in our study was relatively modest and lack of external validation. To confirm our findings, a prospective study with a large cohort of AL amyloidosis patients from multi-center is warranted. Second, some potential key factors may be missed in the medical record or the process of developing the RSF model. Detailed clinical data from patients with AL amyloidosis are also needed. Third, advancements in treatment always result in a better prognosis for patients. In our study, only the treatment regimen adopted at the time of confirmation of AL amyloidosis was collected, which may ignore the potential influence of alternative therapies on the survival of patients. Although treatment options were not included in the Final RSF model, the performance of RSF-therapy also indicated the improvement of RSF model with the entry of therapy, which also needs to be tested.

Conclusions

In summary, our research provides a timely and effective approach to accurately predict the survival time of AL amyloidosis patients based on multi-organ indicators by RSF. The performance of the developed RSF model is great and could be a valuable addition to Mayo staging system to help physicians' decision making.

Supplementary Information The online version contains supplementary material available at <https://doi.org/10.1007/s11739-024-03621-8>.

Acknowledgements The authors would like to acknowledge all statisticians for participating in this study.

Author contributions Y. Xing and S. Sun: Conceptualization; Y. Xing, and J. Zhao: Methodology; X. Li and W. Zheng: Data curation; X. Li and Y. Xing: Writing- Original draft preparation; Y. Xing, X. Li, H. Wu and L. Zhao: Visualization and Supervision. S. Sun: Validation and Writing- Reviewing and Editing.

Funding This work was supported by the National Natural Science Foundation of China (grants number 82170722, 82270715), Key

Research and Development Plan of Shaanxi Province (grants number No.2023-ZDLSF-15), Research topic of clinical application of military medicine in Xijing Hospital (Reference number: JSYYZ05), Clinical research project of Fourth Military Medical University (grants number 2021LC2205), and Postdoctoral Lan Jian Sustentation Fund of the Fourth Military Medical University (grants number lj20220102).

Data availability The data that support the findings of this study are available from the corresponding author upon reasonable request.

Declarations

Conflict of interest The authors declare they have no conflict of interest.

References

- Zanwar S, Gertz MA, Muchtar E (2023) Immunoglobulin light chain amyloidosis: diagnosis and risk assessment. *J Natl Compr Canc Netw* 21(1):83–90
- Quock TP et al (2018) Epidemiology of AL amyloidosis: a real-world study using US claims data. *Blood Adv* 2(10):1046–1053
- Kumar N et al (2022) Global epidemiology of amyloid light-chain amyloidosis. *Orphanet J Rare Dis* 17(1):278
- Staron A et al (2021) Marked progress in AL amyloidosis survival: a 40-year longitudinal natural history study. *Blood Cancer J* 11(8):139
- Palladini G et al (2023) The management of light chain (AL) amyloidosis in Europe: clinical characteristics, treatment patterns, and efficacy outcomes between 2004 and 2018. *Blood Cancer J* 13(1):19
- Muchtar E et al (2017) Improved outcomes for newly diagnosed AL amyloidosis between 2000 and 2014: cracking the glass ceiling of early death. *Blood* 129(15):2111–2119
- Kumar S et al (2012) Revised prognostic staging system for light chain amyloidosis incorporating cardiac biomarkers and serum free light chain measurements. *J Clin Oncol* 30(9):989–995
- Oubari S et al (2024) Daratumumab in first-line treatment of patients with light chain amyloidosis and Mayo stage IIIb improves treatment response and overall survival. *Haematologica* 109(1):220–230
- Kastritis E et al (2021) Daratumumab-based treatment for immunoglobulin light-chain amyloidosis. *N Engl J Med* 385(1):46–58
- Wechalekar AD et al (2023) Guidelines for non-transplant chemotherapy for treatment of systemic AL amyloidosis: EHA-ISA working group. *Amyloid* 30(1):3–17
- Khawaja J et al (2024) Limited utility of Mayo 2012 cardiac staging system for risk stratification of patients with advanced cardiac AL amyloidosis - analysis of a uniformly treated cohort of 1,275 patients. *Haematologica*. <https://doi.org/10.3324/haematol.2023.284348>
- Fotiou D, Theodorakakou F, Kastritis E (2021) Biomarkers in AL amyloidosis. *Int J Mol Sci* 22(20):10916
- Jamet B et al (2021) Random survival forest to predict transplant-eligible newly diagnosed multiple myeloma outcome including FDG-PET radiomics: a combined analysis of two independent prospective European trials. *Eur J Nucl Med Mol Imaging* 48(4):1005–1015
- Bohannan ZS, Coffman F, Mitrofanova A (2022) Random survival forest model identifies novel biomarkers of event-free survival in high-risk pediatric acute lymphoblastic leukemia. *Comput Struct Biotechnol J* 20:583–597

15. Rajkumar SV et al (2014) International Myeloma Working Group updated criteria for the diagnosis of multiple myeloma. *Lancet Oncol* 15(12):e538–e548
16. Gertz MA et al. (2005) Definition of organ involvement and treatment response in immunoglobulin light chain amyloidosis (AL): a consensus opinion from the 10th International Symposium on Amyloid and Amyloidosis, Tours, France, 18–22 Apr 2004. pp. 319–328
17. Collins GS et al (2015) Transparent reporting of a multivariable prediction model for individual prognosis or diagnosis (TRIPOD): the TRIPOD statement. *BMJ (Clin Res Ed)* 350:g7594
18. Garcia-Garcia HM et al (2019) Impact of periprocedural myocardial biomarker elevation on mortality following elective percutaneous coronary intervention. *JACC Cardiovasc Interv* 12(19):1954–1962
19. Jang JG et al (2020) Prognostic factors for severe coronavirus disease 2019 in Daegu, Korea. *J Korean Med Sci* 35(23):e209
20. Brenner DA et al (2004) Human amyloidogenic light chains directly impair cardiomyocyte function through an increase in cellular oxidant stress. *Circ Res* 94(8):1008–1010
21. Ghio S et al (2007) Importance of the echocardiographic evaluation of right ventricular function in patients with AL amyloidosis. *Eur J Heart Fail* 9(8):808–813
22. Wang X et al (2022) Feasibility of (68)Ga-labeled fibroblast activation protein inhibitor PET/CT in light-chain cardiac amyloidosis. *JACC Cardiovasc Imaging* 15(11):1960–1970
23. Gertz MA, Kyle RA (1988) Hepatic amyloidosis (primary [AL], immunoglobulin light chain): the natural history in 80 patients. *Am J Med* 85(1):73–80
24. Park MA et al (2003) Primary (AL) hepatic amyloidosis: clinical features and natural history in 98 patients. *Medicine* 82(5):291–298
25. Rosenzweig M, Kastiris E (2020) Liver and gastrointestinal involvement: update. *Hematol Oncol Clin North Am* 34(6S):e1–e13
26. Borovac JA et al (2020) Right ventricular free wall strain and congestive hepatopathy in patients with acute worsening of chronic heart failure: a CATSTAT-HF echo substudy. *J Clin Med* 9(5):1317
27. Migrino RQ et al (2009) Left ventricular ejection time on echocardiography predicts long-term mortality in light chain amyloidosis. *J Am Soc Echocardiogr* 22(12):1396–1402
28. Ditttrich T et al (2019) Performance analysis of AL amyloidosis cardiac biomarker staging systems with special focus on renal failure and atrial arrhythmia. *Haematologica* 104(7):1451–1459
29. Palladini G et al (2014) A staging system for renal outcome and early markers of renal response to chemotherapy in AL amyloidosis. *Blood* 124(15):2325–2332
30. Jimenez-Zepeda V et al (2023) A comprehensive multidisciplinary diagnostic algorithm for the early and efficient detection of amyloidosis. *Clin Lymphoma Myeloma Leuk* 23(3):194–202
31. Yan W et al (2021) A prognostic staging system for light-chain amyloidosis using hepatic and renal indicator data from 1,064 Chinese patients. *Ann Transl Med* 9(16):1347–1347
32. Taylor JMG (2011) Random survival forests. *J Thorac Oncol* 6(12):1974–1975
33. Dispenzieri A et al (2003) Survival in patients with primary systemic amyloidosis and raised serum cardiac troponins. *Lancet* 361(9371):1787–1789
34. Palladini G et al (2010) The combination of high-sensitivity cardiac troponin T (hs-cTnT) at presentation and changes in N-terminal natriuretic peptide type B (NT-proBNP) after chemotherapy best predicts survival in AL amyloidosis. *Blood* 116(18):3426–3430
35. Kumar S et al (2023) Impact of cytogenetic abnormalities on treatment outcomes in patients with amyloid light-chain amyloidosis: subanalyses from the ANDROMEDA study. *Amyloid* 30(3):268–278
36. Chakraborty R et al (2023) First report of outcomes in patients with stage IIIb AL amyloidosis treated with Dara-VCD front-line therapy. *Br J Haematol* 201(5):913–916

Publisher's Note Springer Nature remains neutral with regard to jurisdictional claims in published maps and institutional affiliations.

Springer Nature or its licensor (e.g. a society or other partner) holds exclusive rights to this article under a publishing agreement with the author(s) or other rightsholder(s); author self-archiving of the accepted manuscript version of this article is solely governed by the terms of such publishing agreement and applicable law.